Low Velocity Elastomer Polymer Wedges Applied to Phased Array Probes

Ed GINZEL [1]
Robert GINZEL[2], Rick MACNEIL [3]
[1] Materials Research Institute, Waterloo, Ontario, Canada e-mail: eginzel@mri.on.ca
[2] Ginzel & Associates Ltd., Williamsford, Ontario, Canada email: rginzel@ginzelassociates.com
[3] Innovation Polymers, Kitchener, Ontario, Canada email: rmacneil@innovationpolymers.ca

Abstract

Phased array refracting wedges are generally made with a natural incidence angle that permits an effective range of refracted angles. Manufacturers suggest that it is useful between about plus or minus 15° from that natural refracted angle. Theory indicates that the range of sweep is based on the -6dB beam spread of the individual elements in the incidence medium. Therefore, the refracted range could be greater than the manufacturer's "recommended" value. When the refracting material is one of low velocity, the steering range in that medium is reduced compared to faster velocities. However; using a lower velocity wedge material would reduce the required incidence angle and could thereby increase the echo-transmittance while also providing a higher velocity ratio which permits a smaller range of incident angles to achieve the same refracted range as observed in higher velocity wedge materials.

Low velocity elastomers are compared to standard hard plastics refracting wedges using phased-array S-scans.

Keywords: Phased-array, polymers, S-scans, ultrasonic

1. Introduction

Phased-array probes are commonly used to provide large volume coverage using a fixed position standoff as the beam is swept through a range of angles. This is the foundation of the sectorial or S-scan. The ratio of the refracting material and the test material dictates the incident angles required by the incident beams. Typically the refraction is made possible by using a wedge material under the probe that provides a natural refracted angle for the plane wave formed when no delays are applied to the active aperture. To avoid the formation of grating lobes, manufacturers typically recommend a limit of plus or minus 15° from that natural refracted angle. Theory [1] indicates that the range of sweep is based on a -6dB beam spread of the individual elements in the incidence medium. When the refracting material is of low velocity, the steering range in the wedge is reduced compared to faster velocities. This effect may be somewhat compensated for when the test material has a higher velocity in that relatively small changes in the incident angle produce larger changes in the refracted angle.

Some [2, 3, 4] have experimented with water-gap and water-membrane options. However, the water-gap option may suffer loss of water-column when working on inclined, rough or overhead surfaces and may also suffer from accumulating air bubbles. Water membrane options can also suffer from air-bubble accumulation and risk loss of couplant due to the normal wear that occurs when using a retaining membrane.

In this paper, the authors examine the use of low velocity elastomers as an alternative to the traditional hard plastic wedge materials.

2. Comparing modelled performances of standard and low velocity wedges

Hard plastics such as poly-methyl-methacrylate (PMMA) or cross-linked polystyrene are commonly used for refracting wedges when working on steels. However, when required to work on lower velocity materials such as polyethylene, the attenuation of the shear mode is so large that only the longitudinal mode is practical. Acoustic velocities of polyethylene materials have been measured in a range of 2100-2600m/s [5]. This presents a problem for the hard plastics because their velocity is essentially the same (or faster) than the material being tested. Figure 3 illustrates the limitations caused by the nose and damping material for a cross-linked polystyrene wedge used on a polyethylene joint. The velocity difference between the wedge and test material in Figure 1 is the same so no refraction occurs, and in some cases the refraction can be negative (i.e. the test material velocity is slower than the refracting wedge).
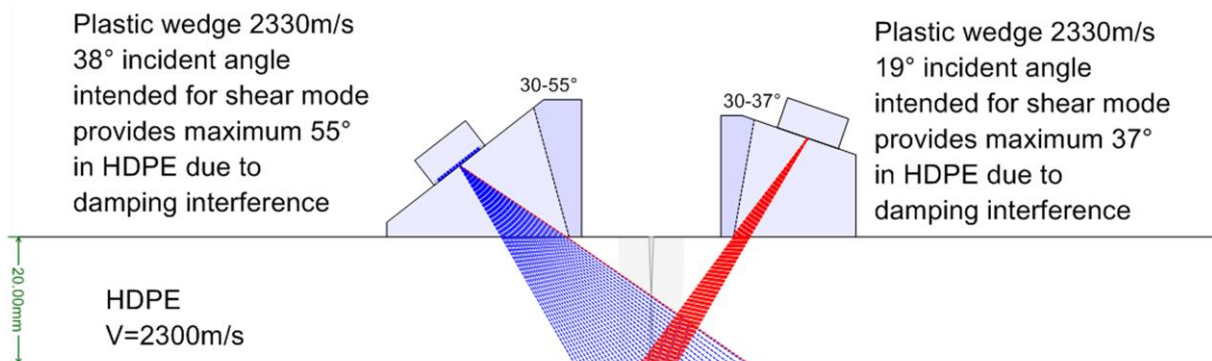

Figure 1   **Limited sweep with hard-plastic refracting wedges on HDPE**

Civa modelling is used to examine the relative sensitivities of a 16 element 0.6mm pitch 5MHz linear phased-array probe using both the standard hard plastic and a low velocity elastomer as the refracting wedge material. The incident angle of the cross-linked polystyrene wedge is 36° and the Aqualene wedge is made at 30°. Delay laws are configured for 55° refracted shear mode in steel for both cases. Figure 2 indicates beam profiles for the two wedge materials on steel.
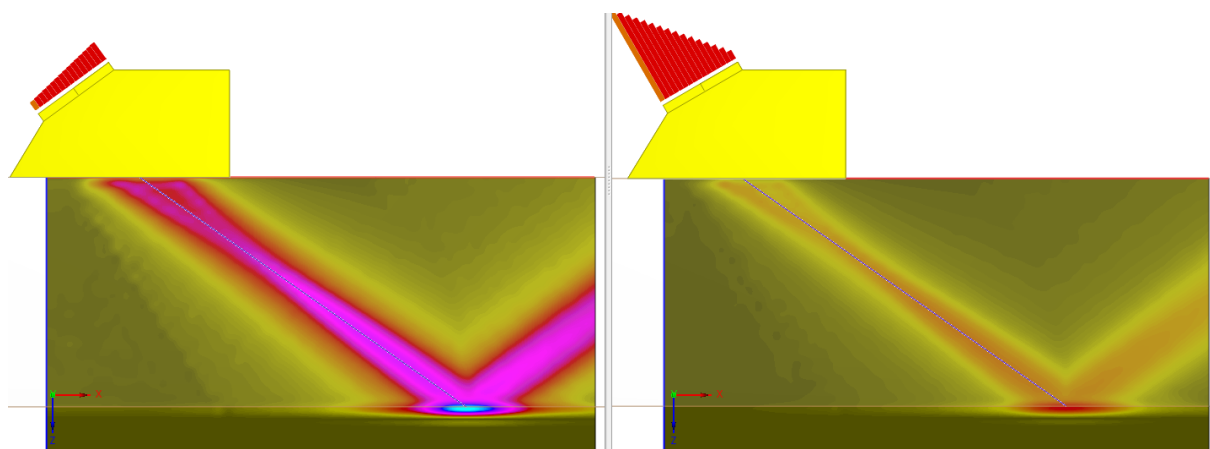

Figure 2   **55° S-mode on Steel – cross-linked polystyrene left, Aqualene right**

The beams were normalised to the polystyrene and we see the beam from the Aqualene wedge as being about 7dB weaker due to the wedge attenuation and reflection effects due to the greater steering of the delay laws.

Figure 3 indicates beam profiles of the same 16 element probe on cross-linked polystyrene and Aqualene as it would perform when placed on high density polyethylene (HDPE).
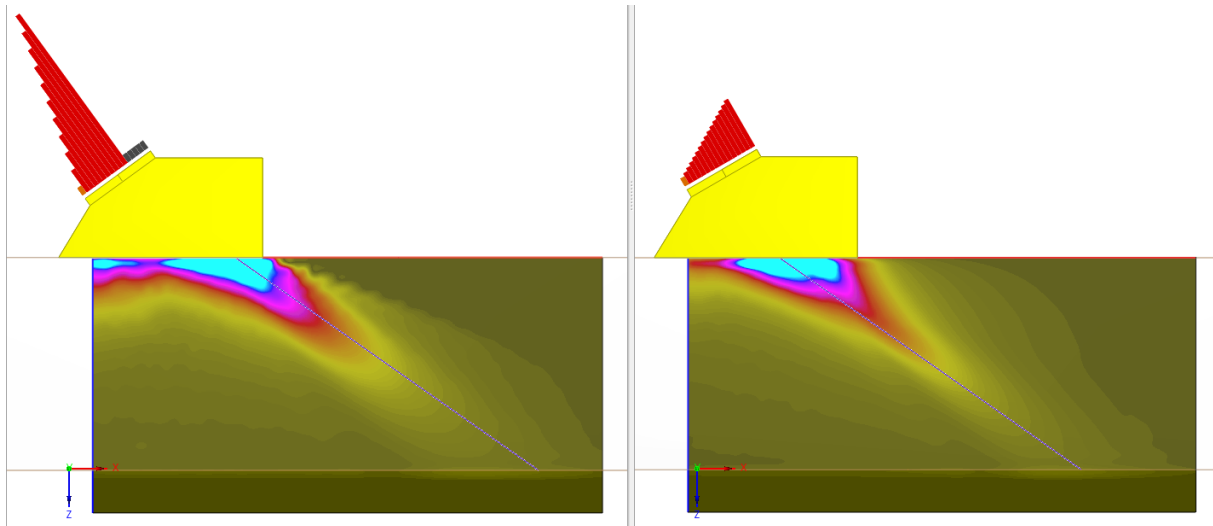

Figure 3   55° L-mode on HDPE – cross-linked polystyrene left, Aqualene right

Figure 3 indicates how the relative on-axis pressures in the HDPE are essentially identical (within 1dB with the Aqualene wedge being slightly more sensitive). What is evident in the case of the HDPE application is that the refraction is limited by the nose of the wedge. Of the 16 elements in the delay law, only 11 are contributing to the beam formation in the case of the polystyrene wedge. In addition to the loss of contributing elements, we can also see that a grating lobe appears at the back of the beam which is not present with the Aqualene wedge.

3 Scanning HDPE targets with elastomer wedges

To validate the modelled responses, a block of HDPE was prepared with side drilled holes (SDHs), flat bottom holes (FBHs) and notches. The cylinder portions of the FBHs were used to establish a TCG and the sensitivity adjusted to obtain a good signal to noise ratio from the tip echoes of the flat bottom surface. The block was a nominal 1 inch thick and measured 26mm.

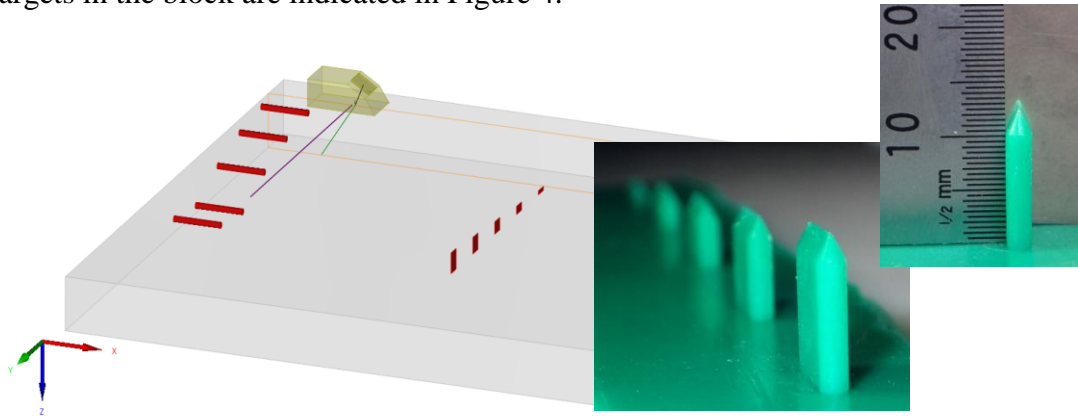Targets in the block are indicated in Figure 4.

Figure 4   HDPE block indicating hole and slot targets

The SDH and FBH targets were 3mm diameter and slots were made with 60° diffraction tips at 1.76, 5.16, 7.34, 10.36 and12.34mm depths. Rubber replicas (seen in Figure 4) were made to verify notch depths to their tips [6]. Earlier work included TOFD inspection of HDPE Butt Fusion welds and as such the notches were produced with V angles to help with evaluation of the diffraction techniques. The compression velocity of the plate was measured to be 2570m/s. The elastomeric materials used for the wedge was Aqualene with a compression velocity of 1566m/s.

4 Aqualene wedge scans

A sectorial scan was configured to sweep from 40° to 80° in 1° increments and the notches on the far side were scanned with sensitivity adjusted to avoid saturating signals. In Figure 5 the Top-Side-End view of the notch scan is shown. The reference cursor is positioned over the 12.34mm notch. The notches are stacked as part of the overlay on the End view (right side) and the upper tip is clearly indicating the correct depth while the lower corner is indicated at the plate thickness. Separation of the upper tip signal from the corner signal is clearly visible for all but the 1.76mm deep notch.
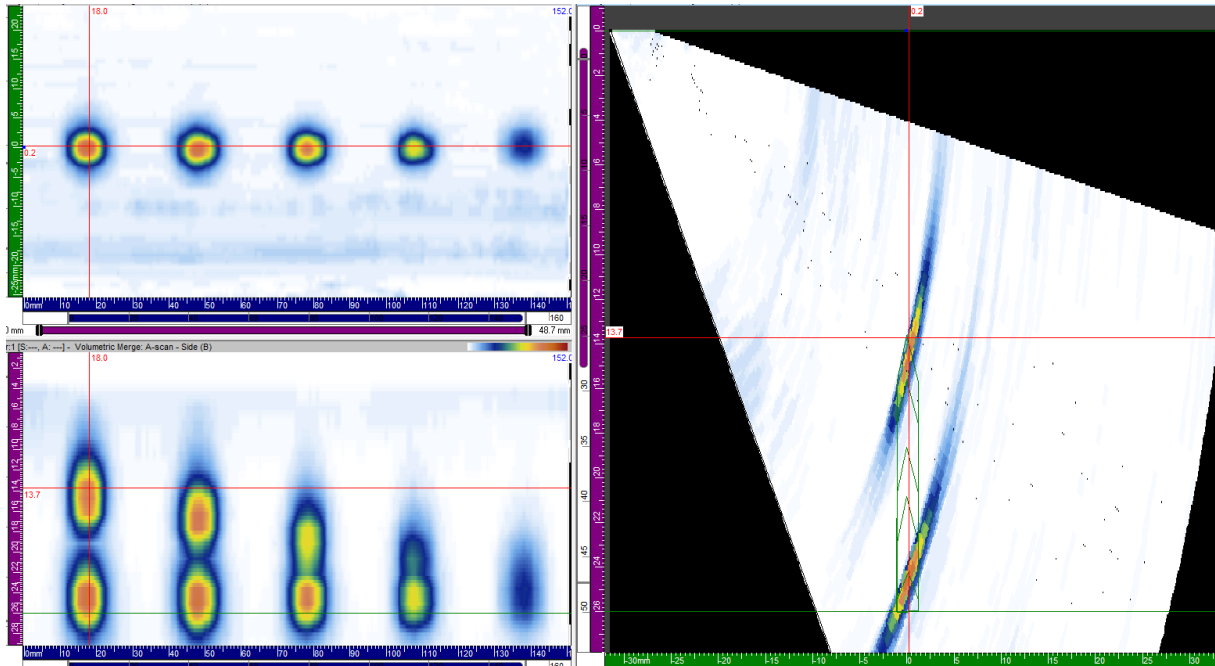
Figure 5   Scan of far surface notches using Aqualene wedge

A slightly different scan setup was used on the FBH targets. This was a sectorial scan from 40° to 85° (also in 1° increments). Figure 6 illustrates the beams formed using the Aqualene wedge for the FBH scan. For the scan of the FBHs, 9dB gain was added to the sensitivity above that used for the notch detection.
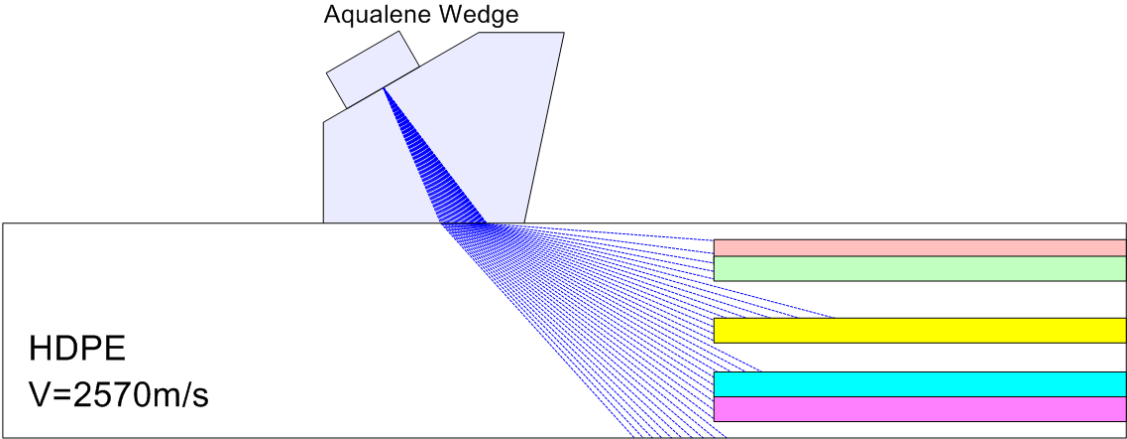

Figure 6   40°-85° S-Scan of FBHs with Aqualene wedge

The Top-Side-End view of the FBHs (Figure 7) indicates good detection of the targets with high signal to noise ratio. What is remarkable is the detection and resolution of the uppermost FBH seen on the left side of the scan image in the Side view (lower left). Not only is the flat bottom hole detected, but it is also indicated as having a ligament. This target was milled with a 2mm ligament between the block surface and the upper tip of the FBH.
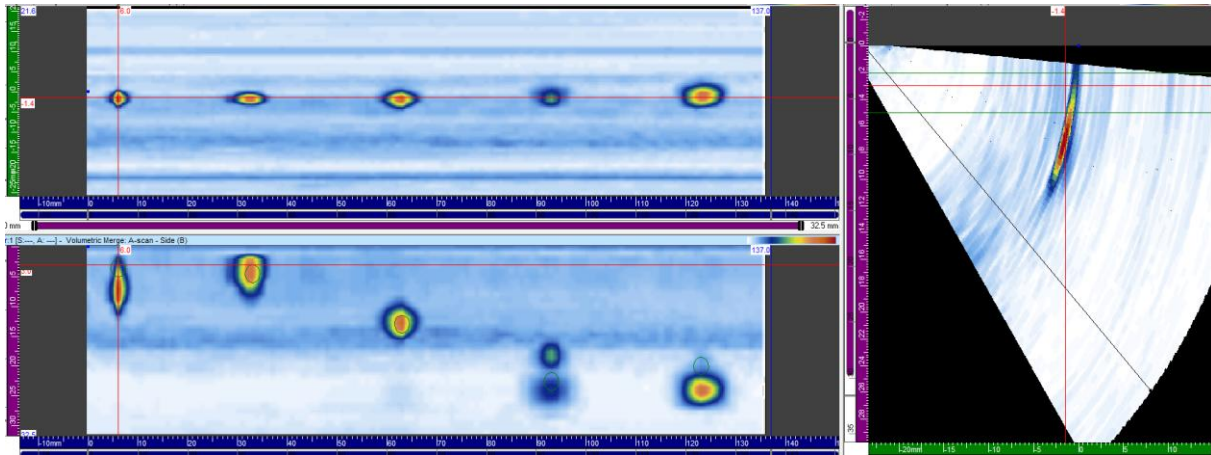
Figure 7   Scan of FBHs using Aqualene wedge

Using the Overlay feature of the software, hole positions were identified on the Side view (Figure 8 red circles). Allowing for the fact that the image is formed by voxelization of the merged data, the first FBH is located within 1.5mm of its correct centre position and the next two FBHs are within 0.5 of their true centre positions.
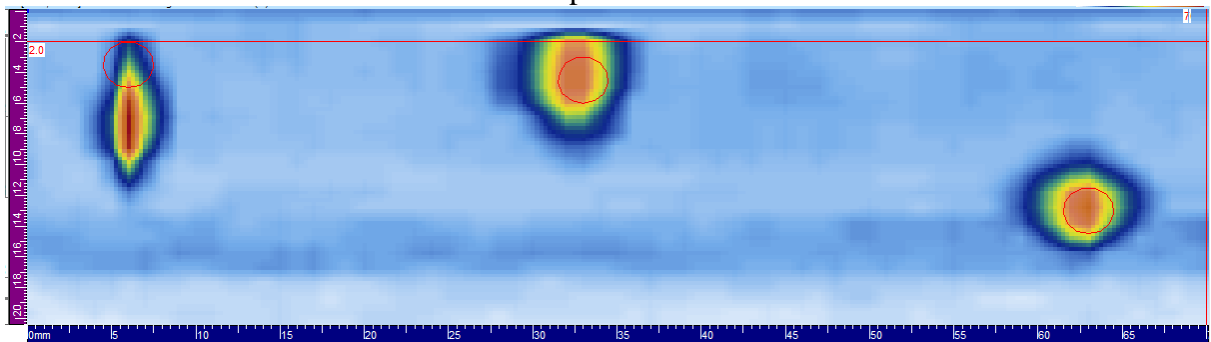

Figure 8   Positioning of FBHs from pulse-echo scan data using Aqualene wedge

The last two FBHs seem to be mis-positioned until the signals are compared to the End view responses (S-scan display). Figure 9 has the reference cursor over the response from the FBH having a small (2mm) ligament from the far surface. The higher amplitude signal (at the crossing point of the red cursors) is well above the actual hole depth. However, there is a slightly lower amplitude signal at the true depth of the FBH.
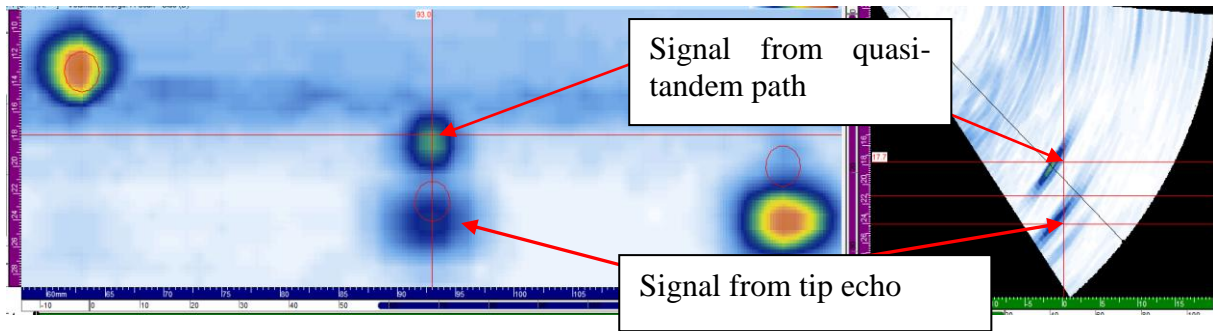
Signal from quasi-tandem path

Signal from tip echo

Figure 9   Quasi-tandem and tip echo sources of FBH with 2mm ligament

The quasi-tandem path that is the source of the larger amplitude signal can be explained by the specular reflection of the beams around 51° refracted angle. These are not direct centre-of-beam paths, but merely the optimum angle for a return path. The black line from the arcs seen in Figure 10 indicate the path from a specular reflection with the 4th FBH.
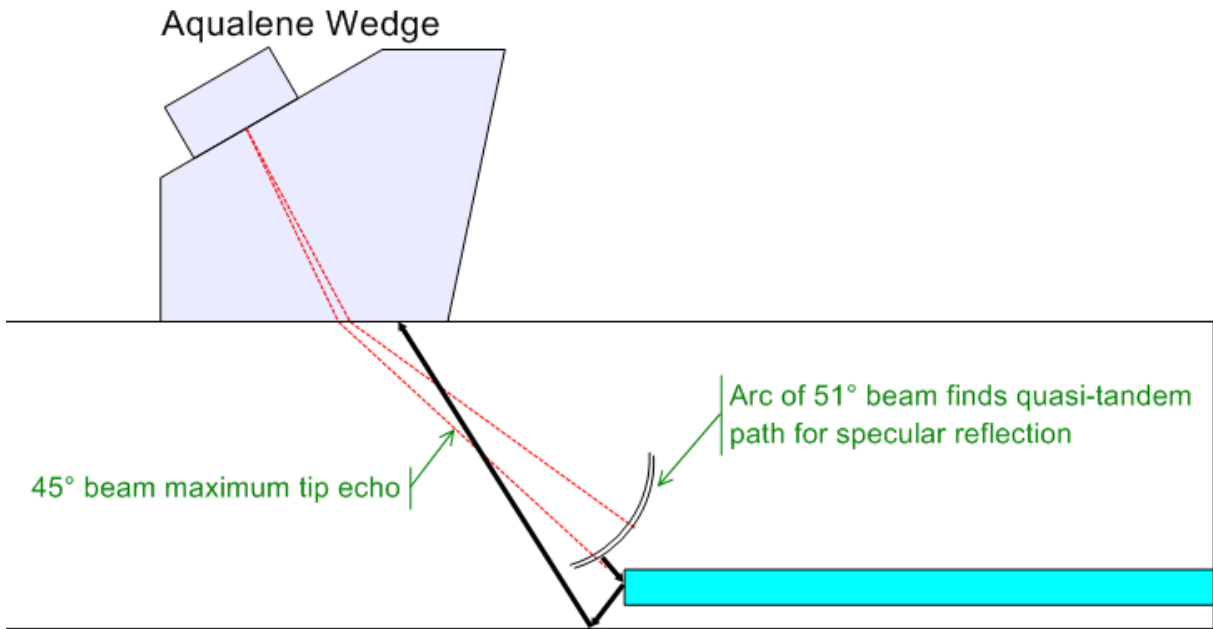

Aqualene Wedge

Arc of 51° beam finds quasi-tandem path for specular reflection

45° beam maximum tip echo

Figure 10   Raytrace for quasi-tandem sources of FBH with 2mm ligament

The slight offset of the 5th FBH is of a similar origin. The colour intensity change is not well seen on the Side view but evidence of the tip echo from the upper part of the FBH is evident on the S-scan. In Figure 11 the three horizontal red lines indicate the top, middle and bottom of the FBH. Maximum signal amplitude is seen below the actual hole position with the 45° beam having made a quasi-tandem path from a specular reflection off the FBH surface and far wall.
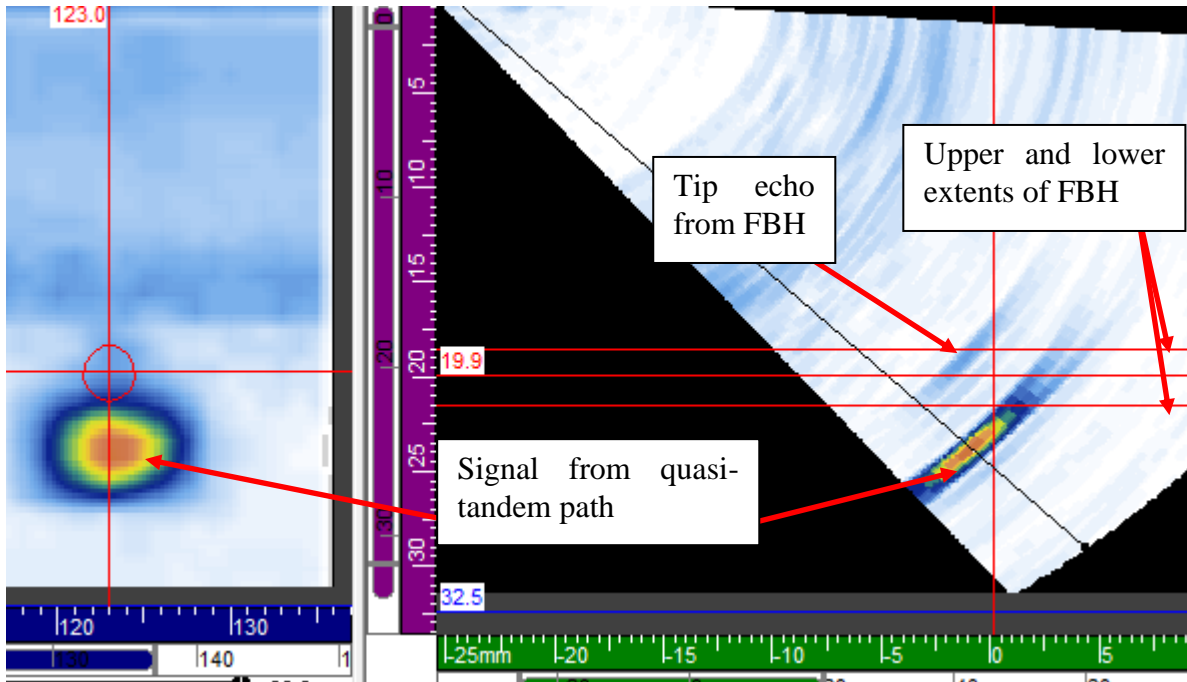
Figure 11   Signals for FBH centred at 20mm from test surface

A scan of the notches from the near surface produces an interesting pattern as seen in Figure 12. The scan in Figure 12 was made using 4dB less than the scan for the FBHs yet the upper signals saturate in all cases except for the shallowest (2mm) notch. Associated with the 4 deepest notches are secondary indications at the depth of the notch.
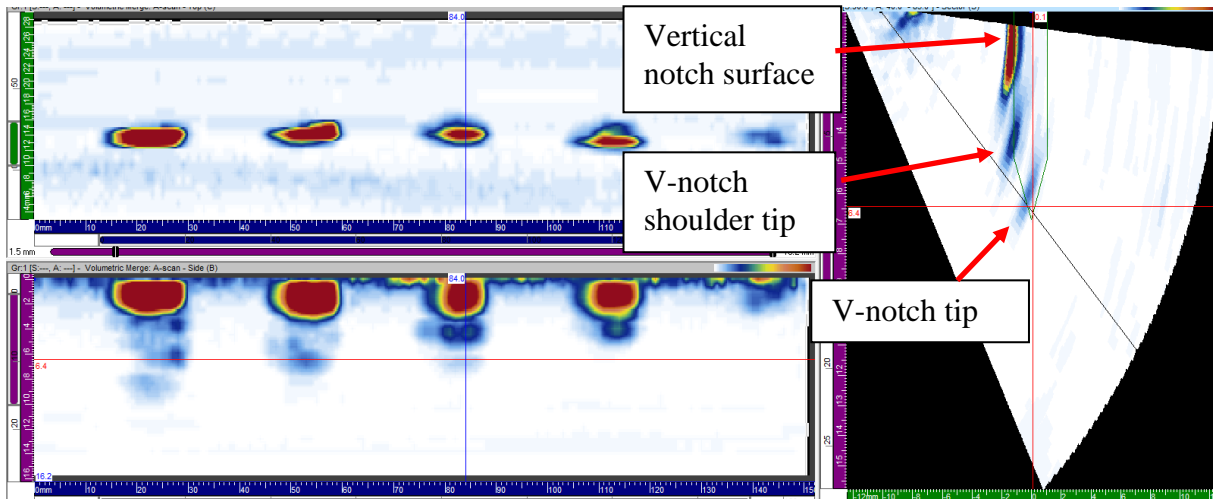

Figure 12   Signals for notches scanned from near surface (S-scan at 8mm notch)

Civa modelling provides an explanation of the signal origins for the near surface-breaking notches. The uppermost vertical portion of the notch accounts for the first arriving signal for the highest angles. A tip effect is had from both the shoulder of the notch at the V as well as the tip of the V.
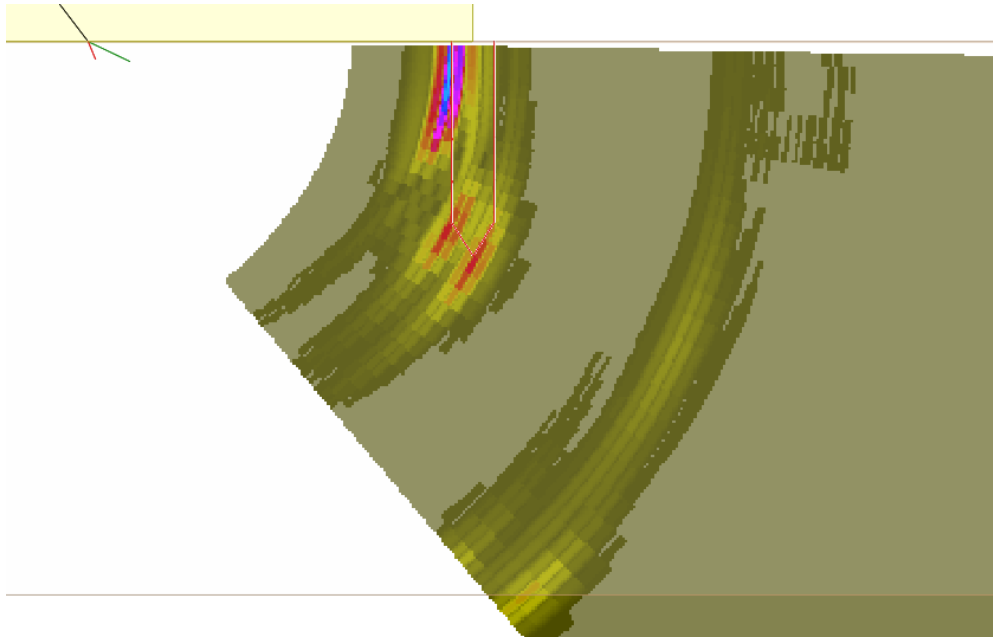
Figure 13   Civa model of signals for 10mm deep V notch

5 Conclusions

Low velocity elastomeric materials provide an effective alternative to water jacketed refracting wedges for phased-array probe applications. They are not impeded by the potential loss of water-column when working on inclined, rough or overhead surfaces. Unlike water column options, the low velocity solid does not suffer from accumulating air bubbles and it does not risk loss of couplant due to failure of the membrane with normal wear that occurs when using a retaining membrane. Good sensitivity and resolution has been demonstrated on standard targets in a relatively lossy HDPE plate.

Several options now exist for low-velocity elastomeric materials with low attenuation suitable for wedges. Future work will be done to optimise the wedge geometry. A future report is planned to demonstrate the concept on butt fusion joints in HDPE piping.

References

1. Introduction to Phased Array Ultrasonic Technology Applications http://www.olympus-ims.com/en/books/ , Published by Olympus NDT, 2007
2. D. Maclennan, I.G. Pettigrew and C.R. Bird, Plastic Fantastic? – An NDE Inspection solution for HDPE butt welds, www.ndt.net/article/jrc-nde2012/papers/152.pdf
3. F. Hagglund, M. Robson, M.J. Troughton, W. Spicer, I.R. Pinson, A Novel Phased Array Ultrasonic Testing (PAUT) System for On-Site Inspection of Welded Joints in Plastic Pipes, www.ndt.net/events/ECNDT2014/app/content/Paper/362_Hagglund.pdf
4. J. Russell, P.Cawley, Development of a Membrane Coupled Conformable Phased Array, http://www.ndt.net/article/jrc-nde2009/papers/108.pdf
5. E. Ginzel, B. Turnbull, Determining Approximate Acoustic Properties of Materials, NDT.net Dec. 2016 http://www.ndt.net/article/ndtnet/2016/17_Ginzel.pdf
6. Ed Ginzel, Robert Ginzel, Rick MacNeil, Low Velocity Elastomer Polymer Wedges Applied to TOFD, NDT.net March 2016, http://www.ndt.net/article/ndtnet/2016/11_Ginzel.pdf